Postural and locomotor control in normal and vestibularly deficient mice

P.-P. Vidal[1], L. Degallaix[1,2], P. Josset[1], J.-P. Gasc[2] and K. E. Cullen[3]

[1]*Laboratoire de Neurobiologie des Réseaux Sensorimoteurs, UMR 7060, CNRS-Paris 5-Paris 7, Paris, France*
[2]*Adaptations et Evolution des Systèmes Ostéomusculaires, UMR 8570, CNRS-Muséum National d'Histoire Naturelle, Paris, France*
[3]*Aerospace Medical Research Unit, Department of Physiology, McGill University, Montréal, Canada*

We investigated how vestibular information is used to maintain posture and control movement by studying vestibularly deficient mice (IsK$^{-/-}$ mutant). In these mutants, microscopy showed degeneration of the cristae of the semicircular canals and of the maculae of the utriculi and sacculi, while behavioural and vestibulo-ocular reflex testing showed that vestibular function was completely absent. However, the histology of Scarpa's ganglia and the vestibular nerves was normal in mutant mice, indicating the presence of intact central pathways. Using X-ray and high-speed cineradiography, we compared resting postures and locomotion patterns between these vestibularly deficient mice and vestibularly normal mice (wild-type and IsK$^{+/-}$). The absence of vestibular function did not affect resting posture but had profound effects on locomotion. At rest, the S-shaped, sagittal posture of the vertebral column was the same for wild-type and mutant mice. Both held the head with the atlanto-occipital joint fully flexed, the cervico-thoracic junction fully flexed, and the cervical column upright. Wild-type mice extended the head and vertebral column and could walk in a straight line. In marked contrast, locomotion in vestibularly deficient mice was characterized by circling episodes, during which the vertebral column maintained an S-shaped posture. Thus, vestibular information is not required to control resting posture but is mandatory for normal locomotion. We propose that vestibular inputs are required to signal the completion of a planned trajectory because mutant mice continued rotating after changing heading direction. Our findings support the hypothesis that vertebrates limit the number of degrees of freedom to be controlled by adopting just a few of the possible skeletal configurations.

(Received 4 March 2004; accepted after revision 2 July 2004; first published online 8 July 2004)
Corresponding author P.-P. Vidal: Laboratoire de Neurobiologie des Réseaux Sensorimoteurs, 45 rue des Saint-Pères, 75270 Paris cedex 06, France. Email: ppvidal@biomedicale.univ-paris5.fr

The vestibular system functions to detect the motion of the head-in-space, and in turn, generate the reflexes that are crucial for our daily activities, such as stabilizing the visual axis (gaze) and maintaining head and body posture (reviewed by Cullen & Roy, 2004). Angular head velocity is detected by vestibular hair cells that are located within the semicircular canals of the inner ear labyrinth. The afferent fibres of the vestibular (VIII) nerve project from the labyrinth directly to the vestibular nuclei of the brainstem. Bilateral loss of labyrinthine functional causes (1) the visual world to move on the retina with head movements, (2) an inability to keep the head/body erect during common activities, and (3) an inability to perform tasks that require spatial orientation such as determining the direction of body motion or navigating through space in the absence of visual cues. Following unilateral vestibular damage in adults, there is evidence that static deficits - including head tilt and spontaneous nystagmus - are readily compensated while compensation for dynamic vestibular deficits is far less complete (reviewed by Vidal *et al.* 1998; Curthoys, 2000; Darlington *et al.* 2002).

To date, the question of whether vestibular deficits in very early stages of ontogeny might alter resting posture and motor control has received surprisingly little attention. Recent developments in mouse genetic engineering, involving the creation of transgenic and knockout mutant mice, have provided a novel opportunity to study the relationship between genes and behaviour. Many mutant mice strains display behavioural phenotypes that are suggestive of a bilateral vestibular dysfunction. In particular, behaviours including head tilting, head tossing, head bobbing, locomotive circling, waltzing behaviours and ataxia are common (summarized as the shaker/waltzer behaviour) in many mutants. However,

 DOI: 10.1113/jphysiol.2004.063883

a causal relationship between the postulated vestibular deficits and the shaker/waltzer behaviour had never been demonstrated because mutations inducing the classic shaker/waltzer behaviour are either widespread in the CNS or unknown. Furthermore, in these studies, mutant vestibular fucntion was never rigorously quantified.

In the present study we focus on mice with a null mutation of the IsK gene, which produces the shaker/waltzer phenotype (Vetter *et al.* 1996). These mice apparently have normal vestibular end-organs at birth but the mutation reduces transepithelial potassium secretion in the inner ear early during postnatal development. This agrees with the IsK gene encoding the beta subunit of delayed rectifier potassium channels (Takumi *et al.* 1988). This causes degeneration of the hair cells and transitional epithelium of the vestibular organs (Nicolas *et al.* 2001). IsK transcripts are present in a variety of tissues including heart and kidney, but are absent in brain (Warth & Barhanin, 2002). Thus, with this peripheral vestibular loss, but probably normal central vestibular pathways, the IsK mutant provides a good model to study how vestibular signals are used to control posture and locomotion.

Methods

Cineradiography

Locomotive behaviour was studied using cineradiography in control and mutant mice. Cineradiography was chosen as it (1) successfully circumvents the masking effect of the soft tissue, thereby providing a direct measure of body motion, and (2) provides temporal and spatial resolution in the order of milliseconds and millimeters, respectively. This latter feature was critical for the study of motor control in this species, as unrestrained mice can achieve very high velocity movements. A digital camera (Motionscope) was used to register sequences of 8 s at 250 frames s^{-1}. This frequency was selected as a compromise between maximum time resolution and the spatial definition required for a frame-by-frame data analysis. The Motionscope was coupled with a cineradiographic apparatus (Philips Medical System). Experimental parameters were fixed at 60 kV, with a field of 25 cm diameter. The frames were stored on-line using custom software (Colorvision I). Unrestrained wild-type (C3H; $n = 3$) and $IsK^{+/-}$ mice ($n = 3$) were placed in a Plexiglass corridor (26 × 7 cm) and filmed from the side as they trotted on a treadmill. The treadmill was set to maximal speed that mice could manage without starting to jump. Motor control in $IsK^{-/-}$ mice could not be investigated using a treadmill as these mice were incapable of generating locomotion in a straight line in an open field. Instead, $IsK^{-/-}$ mice ($n = 3$) were placed in a Plexiglass box (18 × 12 × 7.5 cm) and their spontaneous circling episodes were filmed. Filming was from above, because the bone structures at play during circling were superimposed when viewed from the side. Three episodes of circling, each of five turns, were studied for each circling mouse. The mean velocity of body rotation was determined for each episode and the mean value was then calculated. In addition, supports of various roughness were used to test whether proprioceptive information influenced circling behaviour.

Using sequences of 8 s at 250 frames s^{-1} from above and from the side provided a large mass of data to analyse. However two factors facilitated the quantification of the mice behaviour. First, one frame every 20 ms (that is sampling at 50 Hz) proved to be sufficient to characterize locomotor behaviour. Second, the frame by frame analysis turned out to give very consistent results for the behavioural patterns observed during running and circling from one mouse to another, which allowed us to reduce the study to three mice in each case.

Data analysis was performed off-line, using custom software (Sigma Scan Pro 5). The software facilitated the determination of the Cartesian coordinates of several anatomical markers, which were used to calculate various angles describing the skeletal geometry of the mice during treadmill locomotion and circling. For treadmill locomotion, the coordinates of the incisors base, skull base, cervico-thoracic inflection, dorsal base of diaphragm, and ilio-sacral junction were marked. For episodes of circling, the location of the nose, mandibular symphysis, scapular girdle, extremities of the four limbs, diaphragm and pelvic girdle were marked.

Quantification of resting posture

Resting wild-type mice ($n = 4$), $IsK^{+/-}$ mice ($n = 4$) and $IsK^{-/-}$ mice ($n = 4$) were filmed from the side while standing freely on a platform in a Plexiglass box (15 × 25 × 12 cm). Resting posture was defined as a period of immobile stance lasting more than 7 s. Mice were also filmed from above while under deep anaesthesia (choral hydrate, 250 mg kg^{-1} I.P.) lying on their side in a neutral position and then with the head held by tape at the extremes of ventral flexion, dorsal extension, and lateral flexion. Care was taken to avoid out-of-plane movements during these manipulations.

Film was analysed off-line using various landmarks. The orientation of the horizontal semicircular canal (hscc) plane with respect to the earth horizontal plane was determined using the basi-occipital plane as a landmark structure. By dissection of one skull, a 53 degree angle was measured between the horizontal semicircular canal plane and the basi-occipital plane. Four reference lines were identified on each frame. Line v was perpendicular to the horizontal support (line h) surface and is the reference for gravity. Line s, which describes head orientation, was along the clearly visible palate projection and was

aligned with the basi-occipital plane. Line c joined the ventral borders of the C2 to C6 vertebral bodies. Line t joined the ventral borders of the T4 to T11 vertebral bodies.

All the above-described measurements were made independently by two investigators and the original material was re-examination if there were discrepancies. In addition, the centre of gravity was estimated empirically in three mice. Frozen cadavers were successively suspended by a flexible wire using two different points of fixation (head and hindlimb) and photographed. By definition, the two lines determined by the wire intercept at the centre of gravity of the body.

Histological analysis

Animals were decapitated under deep anaesthesia induced by choral hydrate (0.3 ml, I.P.). Each head was divided along the midline into two parts. The brain was carefully removed, and an opening was made in the upper part of each posterior canal for the fixative to penetrate the inner ear. Next, the hemi-craniums were immersed in formalin. Specimens were subsequently fixed in formalin for 2 days. They were next subjected to 1 day of decalcification, and were then paraffin-embedded for sectioning. Tissue sections of the hemi-cranium were stained with haematoxylin-phloxin-saffron.

Unilateral labyrinthectomy

Three adult $IsK^{-/-}$ and three $IsK^{+/-}$ mice were used in this part of the study. All these experiments were carried out in accordance with the European Communities Council directive of 24 November 1986, and following the procedures issued by the French Ministère de l'Agriculture. All efforts were made to minimize animal suffering, and to reduce the number of animals used. Mice were anaesthetized with halothane and a unilateral lesion was made in the left inner ear with the aid of an operating microscope. The entire length of the ventral edge of the meatus was removed using a retroauricular approach, and the facial nerve was sectioned. The tympanic membrane, malleus and incus were extirpated to expose the pterygopalatine artery caudal to the stapes. This artery was electrocoagulated, the stapes was removed and the round window was opened. The vestibule and the cochlea were completely destroyed using a suction tube. The animals were then released in normal visual conditions for 1 week until compensation of the vestibular static deficits occurred. The eye movements were observed using the operating microscope.

Quantification of vestibular dysfunction

In order to confirm the complete absence of vestibular function in $IsK^{-/-}$ mutant mice, vestibular function was tested using four approaches. (1) The vestibular end organs were examined histological (see section on Histological analysis above). (2) Wild-type and mutant mice were tested using a battery of behavioural tests, which assessed their ability to use vestibular information to control posture and navigation. These tests included: (a) Preyer's reflex and startle to loud unexpected noise; (b) the tail-hanging test, consisting of lifting the mice by the tail (Hunt *et al.* 1987) to test their posture when landing; (c) in order to test the contact inhibition of the righting reflex (Shoham *et al.* 1989; Rabbath *et al.* 2001), mice were placed supine on a horizontal surface and another horizontal surface was then lightly placed in contact with their feet pads; (d) for the air righting reflex test (Ossenkopp *et al.* 1990; Rabbath *et al.* 2001), mice were held supine and dropped from a height of 30 cm onto a foam cushion; and (e) mice were placed in a large container filled with 30 cm of water at room temperature (Gray *et al.* 1988; Rabbath *et al.* 2001). (3) unilateral labyrinthectomy (see section above) was performed in three $IsK^{-/-}$ mice to verify that neither ocular nystagmus nor postural syndromes were induced. (4) The vestibulo-ocular reflex (VOR) was characterized in four $IsK^{+/-}$mutant mice and compared to the reflex responses observed in four $IsK^{-/-}$ littermates. For the latter assessment, mice were surgically prepared for chronic behavioural experiments. All procedures in this section were approved by the McGill University Animal Care Committee, and were in strict compliance with the guidelines of the Canadian Council on Animal Care.

Surgery. A chronic head implant was first constructed so that the animal's head could be restrained during testing. Mice were anaesthetized with an I.M. injection $(0.01\ \text{ml}\ 10\ \text{g})^{-1}$) of a mixture of ketamine ($100\ \text{mg ml}^{-1}$), acepromazine maleate ($10\ \text{mg ml}^{-1}$), xylazine ($20\ \text{mg ml}^{-1}$), and saline in a ratio of 5 : 1 : 2.5 : 1.5, respectively. Anaesthesia was monitored using the flexion withdrawal reflex evoked by toe pinch and additional anaesthetic was given as necessary. An anterior–posterior incision was made on the scalp and the skin was retracted to expose the skull. Three small (M1) stainless steel anchor screws were placed in the skull (frontal and parietal bones), and the head-restraining post was attached to the parietal bone with dental acrylic. Animals were given at least 3 days to recover from the surgery before experiments began.

Data acquisition. To measure the eye movements evoked by vestibular stimulation (e.g. the VOR), the mouse was placed in a cylindrical rodent restrainer, which was fixed to the superstructure of a vestibular turntable. The mouse's head was restrained to align the horizontal semi-circular canals with the horizontal plane (see above).

An ISCAN infrared video system (ETL-200, ISCAN, Burlington MA) with optics modified for the mouse eye (75 mm, F = 1.4, TV lens) was used to monitor eye movements. This system uses proprietary algorithms to compute the centre of the pupil and a reference corneal reflection, and can sample each at 120 samples s^{-1}. Because cornea curvature is greater in the mouse than the human, a series of LEDs (see Stahl *et al.* 2000 for details) was used to distribute illumination over the corneal surface. The eye movements produced by the mice were calibrated as described by Stahl *et al.* (2000) and were verified by rotating the camera about the eye in an anaesthetized mouse. Vestibular stimulation and data storage were controlled by a QNX-based real-time data acquisition system (REX) (Hayes *et al.* 1982). Vestibular turntable velocity was measured using an angular velocity sensor (Watson Inc.). Eye and head movement signals were low-pass filtered at 250 Hz (8 pole Bessel filter), sampled at 1000 Hz, and stored on a hard drive for later analysis.

The head-restrained mouse was rotated in the horizontal plane at frequencies of 0.2, 0.4, 0.8, 1.0 and 2.0 Hz (at $\pm$ 6° s^{-1}, and $\pm$ 20° s^{-1} peak velocity) in darkness. The horizontal eye position data obtained during the sinusoidal head oscillations were digitally low-pass filtered using a 51st order finite-impulse-response (FIR) filter with a Hamming window and cutoff frequency set to 30 Hz ('fir1' function: Matlab Signal Processing Toolbox). Zero-phase forward and reverse digital filtering were employed so that the filtered signal had precisely zero phase distortion. To differentiate eye position signals, the first order backward-difference was calculated. The gain of the VOR, as well as the dynamic 'lag' time of eye motion with respect to head motion, was estimated by least-squares optimization (interior-reflective Newton method) as in eqn (1):

$$E'(t) = (\text{gain}) \times [H'(t - t_d)] + \text{bias} \qquad (1)$$

where $E'(t)$ is eye velocity, $H'(t)$ is head velocity, gain is a constant value, t_d is the dynamic lag time (in ms) of the eye movement with respect to the head movement, and bias is a DC offset, which is usually minimal. Using t_d, the corresponding phase (in degrees) of eye velocity relative to head velocity was calculated (phase $= t_d \times 360°/T$, where $T = 1$/frequency of the applied head velocity; negative values indicate a phase lag). Equation (1) was fit to a minimum of seven cycles at each frequency for each animal. Only data from periods of slow-phase vestibular nystagmus that occurred between quick phases of vestibular nystagmus and/or saccades were included in the analysis. Head-unrestrained $IsK^{-/-}$ mice generated frequent episodes of head bobbing in the pitch axis. The amplitude and frequency of the resultant pitch head movements were measured in four $IsK^{-/-}$ mice using the magnetic search coil technique. A lightweight pre-formed hand-wound wire coil (1.1 mm diameter, copper-beryllium, 60 turns) was attached to a miniature coaxial connector. The coil assembly was pre-calibrated in the system and then attached to a mouse's implant. For the recordings, each mouse was placed in a small enclosure, which prevented it from circling and centred it within a 1-meter diameter magnetic field coil system (CNC Engineering). Methods for data acquisition and filtering were identical to those described above for eye movement signals.

Results

Vestibular function

The effects of the absent IsK gene on the vestibular system were examined by (i) histological examination (ii) a battery of behavioural tests (iii) unilateral labyrinthectomy, and (iv) vestibulo-ocular reflex testing.

Vestibular histology. The semicircular canals were severely abnormal in $IsK^{-/-}$ mutants at 5 months of age. The cristae showed massive degeneration at the level of the hair cells (Fig. 1*A*), as well as in the transitional epithelium. In addition, the core of the cristae, containing the nerve fibres coursing into the cristae to make contact with hair cells, was vacuolated (star, Fig. 1*A*). At this developmental stage, the maculae of the utriculus and sacculus exhibit less striking, but nevertheless significant, signs of degeneration. In contrast, detailed analysis of the vestibular nerve fibres (N, Fig. 1*B*) and cells in Scarpa's ganglion (GG) indicated that there was no degeneration in these structures as compared with wild-type mice (Fig. 1*C*).

Behavioural tests. Adult (postnatal day 90) wild-type mice, $IsK^{+/-}$ and $IsK^{-/-}$ mice from the same litter were subjected to six qualitative behavioural tests to identify responses to vestibular and auditory inputs. The wild-type and IsK^{+}-responses were appropriate for normal vestibular and auditory function whereas, in every test, the $IsK^{-/-}$ responses were abnormal. These included: (i) absent Preyer's reflex, (ii) absent startle reflex to loud noise, (iii) posturing for an occipital rather than a forepaw landing when hung by the tail, (iv) inhibition of righting when supine by cutaneous input to the feet, (v) landing on the back when dropped supine and (vi) inability to swim. In addition, we sought early signs of vestibular deficits by examining newborn mice. As early as postnatal day 7 the $IsK^{-/-}$ pups showed signs of lost vestibular function compared with the wild-type and $IsK^{+/-}$ pups.They more often rolled on their backs spontaneously, had greater difficulty righting themselves when put on their backs, and they could not swim.

Unilateral labyrinthectomy. Unilateral labyrinthectomy in three adult IsK$^{-/-}$ and three IsK$^{+/-}$ mice demonstrated the lack of vestibular function in the IsK$^{-/-}$ mutants. Following unilateral labyrinthectomy, the IsK$^{+/-}$ mice displayed ocular nystagmus and static postural syndromes of the type seen in all quadrupedal vertebrate (de Waele *et al.* 1990). In contrast, the IsK$^{-/-}$ mice displayed neither ocular nystagmus nor any static postural syndrome. In addition, IsK$^{-/-}$ mice continued circling following surgery. These findings strongly suggest that the normal spontaneous discharge of vestibular axons is absent in the IsK$^{-/-}$ mice because labyrinthectomy would have interrupted this tonic activity and produced oculomotor and postural changes.

Vestibulo-ocular reflex. Figure 2*A* shows eye and head position recordings from the IsK$^{-/-}$ and control IsK$^{+/-}$ mice for two frequencies. Head rotation elicited compensatory slow-phase eye movements from the IsK$^{+/-}$ mouse but elicited no eye movement in the IsK$^{-/-}$ mouse. At lower frequencies, Isk$^{+/-}$ mice also generated vestibular quick phases (arrow, Fig. 2*A*) but these also were not seen in the IsK$^{-/-}$ mice. It is important to note that recordings of eye movements from IsK$^{-/-}$ mice in the dark while they were stationary did not show spontaneous abnormal eye movements that would indicate a central abnormality.

For IsK$^{+/-}$ mice, the gains of the VOR at both velocities increased linearly with frequency ($P < 0.01$) reaching values near 0.8 at 2 Hz and the phase lag decreased with increasing frequency ($P < 0.02$), approaching 0° lag at 2 Hz (Fig. 2*B*). This VOR frequency response is similar to those previously reported for wild-type mice (Iwashita *et al.* 2001; Stahl, 2002). In contrast, VOR gain in the IsK$^{-/-}$ mice was negligible and statistically insignificant at all frequencies and both velocities. Accordingly, it was not theoretically possible to obtain a reliable phase estimate of the IsK $^{-/-}$ VOR response.

Posture

Resting posture. X-rays were taken while the mice were at rest; that is, alert but stationary. The IsK$^{-/-}$ mice displayed intermittent episodes of head bobbing in which the head oscillated in the sagittal plane about the atlanto-occipital joint by 10–30° at 3–5 Hz. The analysis of resting posture for these mice was therefore limited to periods during which the mice looked straight ahead and the head did not move.

As is shown in Fig. 3, the skeletal configuration during of resting mice was remarkably stereotyped and a typical skeletal profile is shown in Fig. 3. Specifically, in the alert state, the clear S-shaped resting posture was adopted by both wild-type and mutant strains. To quantify this observation, we computed the angles that characterized resting posture using the landmarks illustrated in Fig. 3. These were compared by ANOVA for the wild-type, IsK$^{+/-}$ and IsK$^{-/-}$ mice. This mouse category had no significant

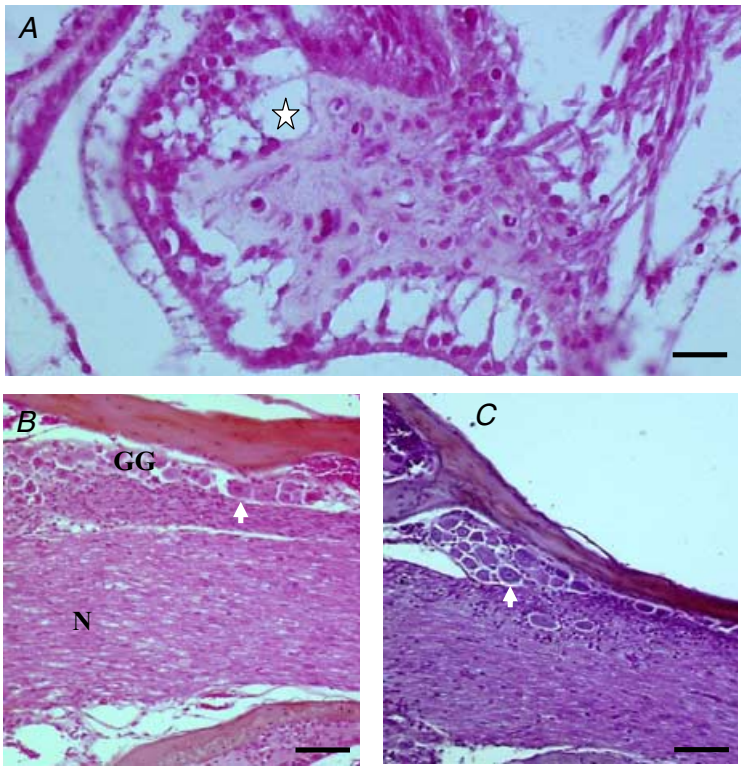

Figure 1. Histology of the IsK$^{-/-}$ vestibular organs
A, crista of the semicircular canal in an IsK$^{-/-}$ mouse. Note the massive degeneration of the hair cells and the vacuoles in the core of the crista (star). The vestibular ganglion and vestibular nerve in the same IsK$^{-/-}$ mouse (*B*) and in a wild-type mouse (*C*). The intact nerve fibres (N) course towards the cristae and the maculae to make contact with hair cells. The soma of the first-order vestibular neurones (arrows), illustrated as a column of cells on the top of *B* and *C*, are intact. Scale bars, 30 μm.

effect on the angles ($F_{2,57} = 0.25$; $P = 0.78$). Mean angles for all 12 mice are shown in Fig. 3. On average, the cervical and thoracic columns were aligned relatively close to vertical in the sagittal plane (lines c and t, Fig. 3). The cervical column leaned $25.0 \pm 5.8^\circ$ forwards of the gravitational vertical and the thoracic column leaned $19.6 \pm 4.5^\circ$ backwards of it. From the top view, deviations in the roll plane were not seen in any of the 12 mice so it appeared that the cervical column is held vertical in the frontal plane.

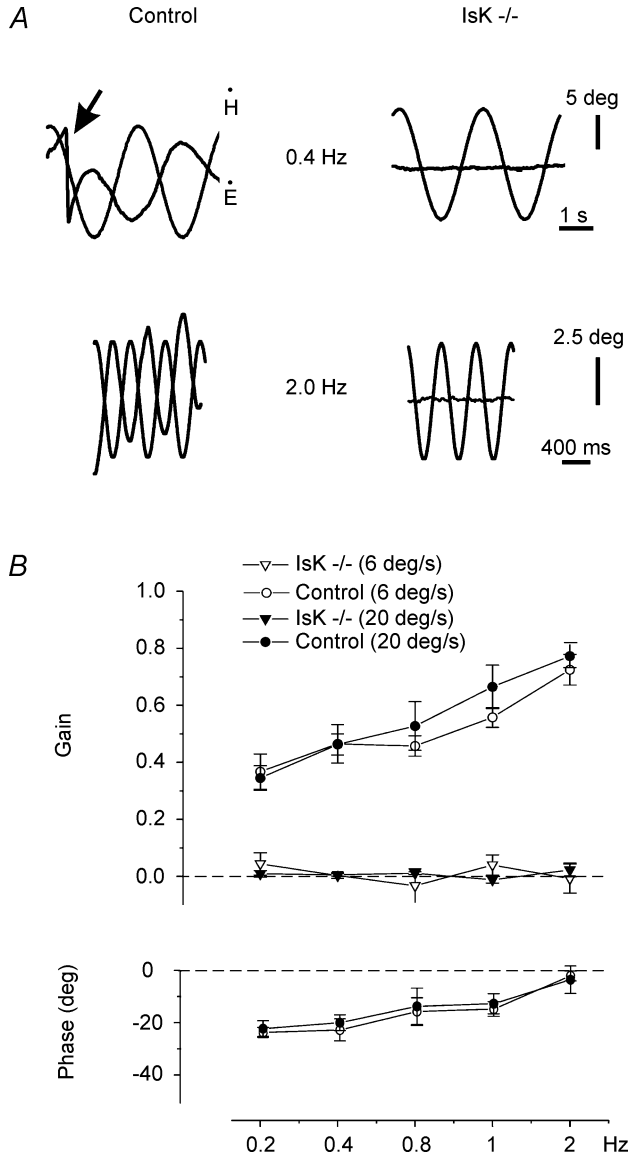

Figure 2. Vestibulo-ocular reflex
A, eye movements evoked during sinusoidal head rotations at 0.4 and 2.0 Hz for a control mouse and an IsK$^{-/-}$ mouse. *B*, mean gain and phase plots of the vestibulo-ocular reflex evoked by 0.2–2.0 Hz rotations in the dark. In normal mice, gain increased linearly with frequency while phase lag decreased with frequency. Responses were the same for stimuli with maximal velocities of 6 or 20° s^{-1}. The VOR gain of IsK$^{-/-}$ mice was zero for all frequencies and both velocities.

Passive posture. To determine the neutral skeletal geometry that would be produced just by passive viscoelastic forces, the mice were anaesthetized and placed on one side for profile X-rays. Mouse category again had no significant effect on the angles ($F_{2,45} = 0.54$; $P = 0.58$). The atlanto-occipital joint angle (∠sc, Fig. 3) was $93.1 \pm 5.4^\circ$ and the cervico-thoracic junction angle (∠ct) was $94.6 \pm 19.1^\circ$.

Range of movement. To measure the range of movement, X-rays were taken while the heads of the anaesthetized mice were held in extreme flexion, extension and lateral flexion. In the sagittal plane, maximal flexion of the atlanto-occipital joint was $71.9 \pm 5.6^\circ$ and the total range of movement was 79.5°. At the cervico-thoracic junction, the maximal extension was $44.1 \pm 5.2^\circ$ and the total range was 109°. The mean range of head rotation in the earth horizontal plane about the longitudinal axis of the cervical column was $\pm 88^\circ$. This arose through excursions at the atlanto-axial joint (aa, Fig. 3) and the cumulative effects of the small axial rotations of the upper cervical vertebrae. Little if any lateral flexion was possible within the structure of the cervical column proper between C2 and C6.

Stabilizing the head. When alert and at rest, all mice held the atlanto-occipital joint near the extreme point of flexion (∠cs, Fig. 3). The mean position of the atlanto-occipital joint ($79.1 \pm 7.9^\circ$) was just 7.2° short of maximal flexion ($71.9 \pm 5.6^\circ$). The head was not held near the neutral position of viscoelastic forces ($93.1 \pm 5.4^\circ$), which was measured in the anaesthetized relaxed mice. With the head in this position at rest, further flexion cannot be used to tilt the head downward. Thus, we observed that head movements were instead generated by flexion at the cervico-thoracic junction (ct, Fig. 3).

The cervico-thoracic junction was held hyper-extended (∠ct, Fig. 3). The mean position of the cervico-thoracic angle was ($43.8 \pm 6.7^\circ$), the same as the measured maximal extension ($44.1 \pm 5.2^\circ$). Again, this was far from the neutral position ($94.6 \pm 19.1^\circ$), measured in the anaesthetized relaxed mice. As upward head movements cannot be produced by extension of the already extended cervico-thoracic junction, we observed that they were produced by extending the atlanto-occipital joint. The sagittal alignments of the cervico-thoracic and atlanto-occipital joints were such that the plane of the horizontal semicircular canal was pitched upwards from the horizontal by $15.4 \pm 4.8^\circ$ (hssc, Fig. 3). In addition, the cervical column was held vertical in the anterior plane. As the cervical column proper between C2 and C6 allows

almost no lateral bending, we observed that stabilizing the head in the roll plane took place at the cervico-thoracic junction about the axis of the C7–T2 vertebrae, an axis close to earth horizontal.

Locomotion

Wild-type and IsK$^{+/-}$ mice could run in a straight path. In contrast, IsK$^{-/-}$ mice could not walk or run in a straight path in an open field or on a treadmill and their locomotion was characterized by episodes of circling interrupted by periods of rest. Frame sequences captured at 250 Hz are shown for both behaviours in Fig. 4.

Running of wild-type and IsK$^{+/-}$ mice. The sequence of limb motion during linear progression was: left forelimb, right hindlimb, right forelimb, then left hindlimb (Figs 4*A* and 5*A*). This 'lateral sequence' pattern has the progression of a hindlimb followed by the ipsilateral forelimb. It is the most common gait pattern among mammals and secures a stable support during locomotion (Renous, 1994). While running on the treadmill, these mice adopted a skeletal configuration in which they held the head in the same orientation in space as at rest with the horizontal semicircular canal plane pitched upward by approximately 15° (Figs 4*A* and 5*B*). The atlanto-occipital joint and the cervico-thoracic junction were fully extended, that is, the neck was lowered so that it was slightly above and approximately parallel to the earth horizontal plane (Fig. 4*A* and 5*C*). The atlanto-occipital joint and the cervico-thoracic junction were fully extended and the thoraco-lumbar kyphosis decreased markedly relative to rest (compare Fig. 3 with Fig. 4*A*).

A remarkable feature of this behaviour was the stability of the head and entire column relative to space. The mean vertical displacements in of the pelvis, diaphragm, skull, scapula or snout never exceeded 3 mm (Fig. 5*D*). In particular, there was no obvious oscillation of the thoraco-lumbar column (Fig. 5*D*) related to the pattern of limb movements (Fig. 5*A*).

Circling of IsK$^{-/-}$ mice. The IsK$^{-/-}$ mice exhibited episodes of spontaneous circling that was randomly either clockwise or counterclockwise. Figure 4*B* illustrates a mouse in typical counter-clockwise rotation. The mean angular velocity of three mice over five consecutive 360° turns was 780° s^{-1}, the peak in one mouse was

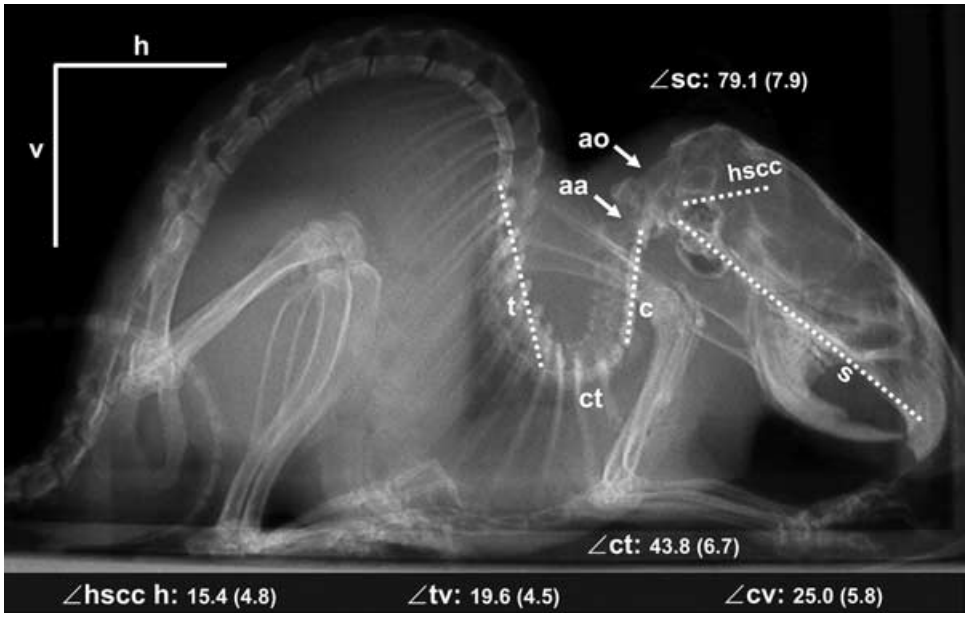

Figure 3. Mouse at rest
The S-shaped configuration is readily apparent. Landmarks used to quantify posture are: t, line of the ventral surfaces of the T4-T11 vertebral bodies; ct, cervico-thoracic junction at C7-T4; c, line of the ventral surfaces of the C2–C6 vertebral bodies; aa, atlanto-axial joint; ao, atlanto-occipital joint; hssc, plane of the horizontal semicircular canal; s, palate projection (aligned with the basi-occipital plane); v, vertical; h, horizontal. Mean ($n = 12$) angles in degrees (S.D) are: ∠sc, skull to cervical spine; ∠ct, cervical to thoracic spine; ∠cv, cervical spine to vertical; ∠tv, thoracic spine to vertical.

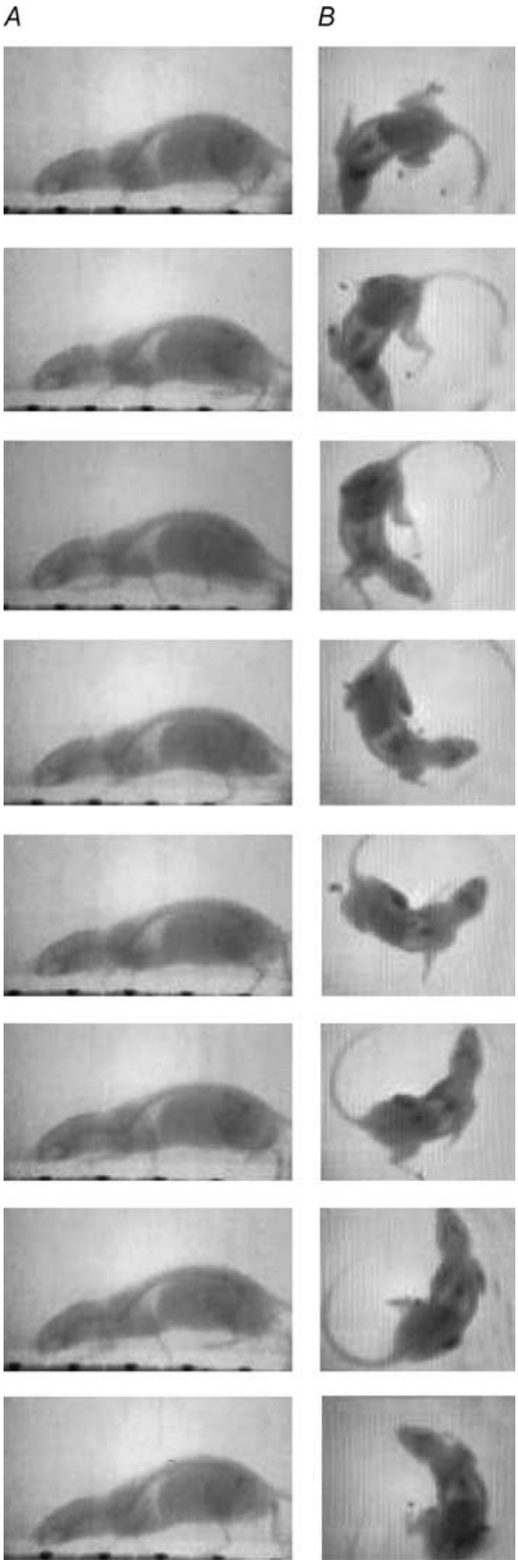

an impressive 968° s^{-1}. During circling, three of the four limbs were synchronized as illustrated in Fig. 4*B* and schematically represented in Figs 6*A* and 7*A*. These included RF, RH and LF, which correspond to the external forelimb, external hindlimb, and internal forelimb with respect to the rotation. The gait sequence was: internal forelimb, external hind limb and external forelimb (Figs 6*A* and 7*A*). The internal hindlimb (LH, Fig. 6*A*) was uncoupled from the stance or swing phases of the three other limbs and executed cycles of variable durations. The external hindlimb (RH) had the largest excursions and highest velocities (~13 cm s^{-1}) while on the other side the internal hindlimb moved little and acted as a pivot (LH in Figs 6*A* and 7*A*), operating independently of the other limbs. In summary, the inner hindlimb acted as a pivot while the outer hindlimb turned about the pivot. The forelimbs produced alternating left right movements just to keep the front of the body in pace. However these movements were not 180° out of phase as for they were for the running mice (Figs 4*A* and 5*A*).

By placing circling mice on glass, wood and sand paper surfaces, we observed that if the foot of the pivoting limb could rotate by slipping on the ground the swing phase became shorter and the stance phase longer. On the glass support, the swing phase was nearly absent. The circling mice placed the pivot foot (LH, Fig. 7*A*) under the diaphragm (dia, Fig. 7*B*). It is worth noting that the diaphragm corresponds to the centre of mass of the mouse body, which suggests that the mice may organize this circling behaviour so that the centre of rotation coincided with the centre of mass of the body.

In the sagittal plane, circling $IsK^{-/-}$ mice adopted the same characteristic S-shaped curve of the cervical, thoracic and lumbar columns as was seen in all mice at rest (Fig. 3). As during rest, the cervical column was pitched forward by about 25°, approximately the angle of line c in Fig. 3. This skeletal geometry sharply contrasted with the column extension during running in a straight line (Fig. 4*A*). To quantify the differences between rest, trot and circling, the projections of the cervical (C), thoracic (T) and lumbar (L) segments onto the horizontal plane were calculated as a percentage of the projection of the entire column. These were similar for rest (C, 10%; T, 39%; L, 51%) and circling (C, 11%; T, 40%; L, 49%), but were different for running (C, 25%; T, 35%; L, 40%) during which the cervical contribution increases.

In the horizontal plane, the head rotated (yaw) about its mid-position by no more than ± 8° (Fig. 6*B*) despite a

Figure 4. Trotting and circling
Cineradiography film captured at 250 Hz and data sampling at 50 Hz. *A*, profile view of an $IsK^{+/-}$ mouse trotting on a treadmill. Note the extension of the whole column. B, view from above of a circling $IsK^{-/-}$ mouse. Note the alternate extension of the forelimbs and hindlimbs.

measured possible range of movement of ± 88°. Rotation of the skull in the pitch or roll produces asymmetrical displacement of the cranial sutures on an X-ray film taken from above. This provided a means of measuring rotation in the sagittal or frontal planes. However, these sutures remained symmetrical indicating that that head bobbing was not present during circling. Thus, the skull remained positioned horizontally relative to the support surface and rotated very little in the horizontal plane. We saw a similar behaviour at the cervico-thoracic junction. Like the cervical vertebrae, thoracic vertebrae can rotate on each other around their longitudinal axis. Because the thoracic column is nearly vertical when IsK$^{-/-}$ mice circle (as at rest, see Fig. 3), it could have acted as a pivot for rotation of the head–neck ensemble. However, the angle between the cervical and thoracic columns maintained a remarkably constant 135° throughout the rotations (Fig. 6*C*). In contrast, between the thoracic and lumbar columns, large oscillatory horizontal movements between 120° and 160° occurred in phase with the cycle of the hindlimb external to the rotation (Fig. 6*D*). The thoraco-lumbar flexed (smaller angle) when the limb was in contact with the ground and exerted its thrust and then extended shortly before the hindlimb left the ground. Thus we see three characteristics of the skeletal configuration in the horizontal plane during circling: head rotation about the cervical column is minimal, a fixed angle is maintained between the head–neck ensemble and the thoracic column, and large oscillatory movements occur between the thoracic and the lumbar columns.

Discussion

The results above show that the resting postures adopted by control and IsK$^{-/-}$ mice were comparable. This finding implies that vestibular information is not crucial for the development of the stereotyped configurations that characterize resting posture. In contrast, locomotion in IsK$^{-/-}$mice was characterized by episodes of circling suggesting that vestibular information was mandatory for providing a reference for head position during locomotion in an open field.

Vestibular function and resting posture

Our results show that, IsK$^{-/-}$ mice totally lack vestibular sensory inputs and yet adopt the same S-shaped posture as wild-type mice at rest. In addition, we demonstrate that this posture is not simply ensured by the passive mechanical properties of the body as the posture in the anaesthetized state is different from that in the alert mice. Hence, a central command is required to maintain an adequate level of tonic muscle activation to ensure the stereotyped skeletal geometry at rest in wild-type and IsK$^{-/-}$ mice (Macpherson, 1998; Fung & Macpherson, 1999; Statler & Keshner, 2003). Taken together, our findings are consistent with the conclusion that vestibular afferent inputs are not mandatory for the determination and the maintenance of the resting posture *per se*. We propose that, when vestibular information is lacking, the integration of inputs from other sensory modalities contributes to the construction of the egocentric frame of reference required for resting posture. On the other hand IsK$^{-/-}$ mice were unable to maintain a stable orientation, with respect to the surface, when attempting to swim. This suggests that (i) vestibular information is required to orientate mice in the absence of proprioceptive inputs from the legs and (ii) in mutant mice, proprioceptive afferent signals substitute for the missing vestibular information to help maintain an S-shaped posture relative to the gravity vector on the ground (see below).

In the three strains of mice, as in all species we have investigated so far at rest (see Table 7 in Graf *et al.* 1995*a*), the plane of the horizontal canals was pitched at an angle of 15.4° up from horizontal; the absence of vestibular function in IsK$^{-/-}$ mice did not result in a different orientation of the head in space compared to the wild-type and IsK$^{+/-}$ mice in between the intermittent episodes

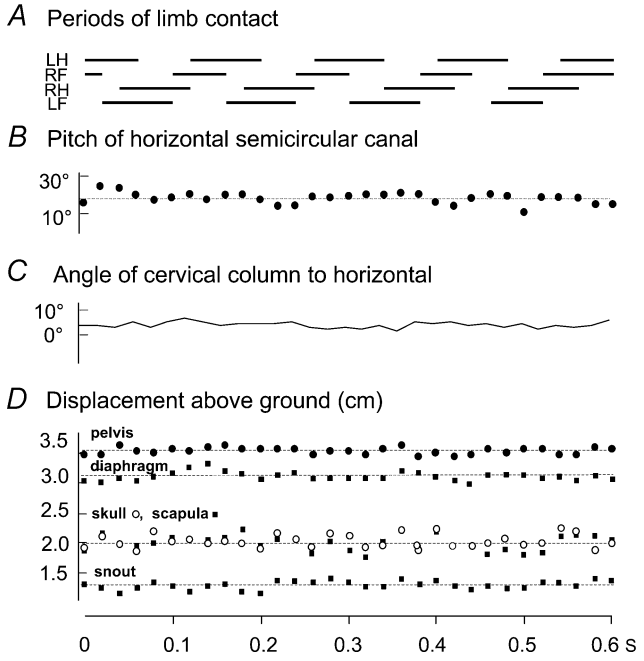

Figure 5. Skeletal geometry of the running IsK$^{+/-}$ mouse
The mouse is running on a treadmill with a mean velocity of 0.52 ms^{-1}. Cineradiography film captured at 250 Hz and data sampling at 50 Hz. *A*, pattern of limb movement of one mouse. The lines indicate the periods of limb contact with the support. LH, left hindlimb; RF, right forelimb; RH, right hindlimb; LF, left forelimb. *B* and *C*, angles of the horizontal semicircular canal and the cervical column to the horizontal earth plane in the same mouse. *D*, mean ($n = 3$) vertical displacements of the pelvis, diaphragm, skull, scapula and snout (base of incisors) above the ground.

of head bobbing. This result suggest that proprioceptive information can substitute for missing vestibular afferent inputs to correctly orientate the cervicothoracic junction and the atlanto-occipital in the sagittal plane so that the head is correctly positioned. However, it is important to emphasize that the vestibular deficits in IsK$^{-/-}$ mice are not limited to the horizontal plane. Performance during the tail-hanging test, the contact inhibition of the righting reflex, the air righting reflex test and the swimming impairment confirm the lack of otolith and vertical canal inputs in IsK$^{-/-}$ mice as in the circling rat (Rabbath *et al.* 2001; Fagerstedt *et al.* 2001). These deficits most probably underlie the constant head bobbing which we observed in the mutants. It is interesting that the head bobbed in the sagittal but not in the horizontal plane, and also at the atlanto-occipital level (ao, Fig. 3) but not at the cervico–thoracic junction (ct, Fig. 3). Thus, taken together our results suggest that vestibular information is not mandatory during development to stabilize the head in the horizontal plane and the neck in the sagittal and frontal planes.

Vestibular function and movement control

In IsK$^{-/-}$ mice one can establish a causal relationship between bilateral degeneration of the vestibular sensors during development and enduring deficits in motor control. This is important, as the question of whether circling is a direct consequence of peripheral vestibular defects has remained a matter of debate (see Kaiser *et al.* 2001). For example, it is not known whether or not the CNS is spared in many mutant mice that demonstrate a circling phenotype (reviewed in Rabbath *et al.* 2001). It is important to note that the IsK transcripts are present in a variety of tissues including heart and kidney, but they are absent in brain (Vetter *et al.* 1996; Warth & Barhanin, 2002). Hence, IsK$^{-/-}$ mice provided a unique opportunity to address this question.

Our results show that wild-type mice perform a symmetrical gait at 0.5 m s^{-1}, characterized by an equal time lag between the lay-down of the hindlimbs and forelimbs. As diagonal limbs land almost simultaneously, and lateral ones are in phase opposition, mice are by definition trotting (Renous, 1994). In contrast, IsK$^{-/-}$ mice generated episodes of circling and were incapable of following a linear trajectory. Circling in IsK$^{-/-}$ mice is likely to be the result of the degeneration of the horizontal semicircular canal sensors. Several arguments support that hypothesis: (i) at 2 months of age, the IsK$^{-/-}$ crista ampullaris appears as an empty shell (Vetter *et al.* 1996); (ii) lack of degeneration of the first order vestibular neurones strongly suggests that central vestibular network remains intact in IsK$^{-/-}$ mice, consistent with lack of evidence for IsK transcripts in brain (Warth & Barhanin, 2002); (iii) guinea pigs circle following selective lesions of the horizontal semicircular canals (de Waele *et al.* 1989); and (iv) bilateral destruction of vestibular hair cells in cat can lead to episodes of bilateral circling (Wersäll & Hawkins, 1962). Consistent with prior studies (Vetter *et al.* 1996; Letts *et al.* 2000) circling by the IsK$^{-/-}$ mice was

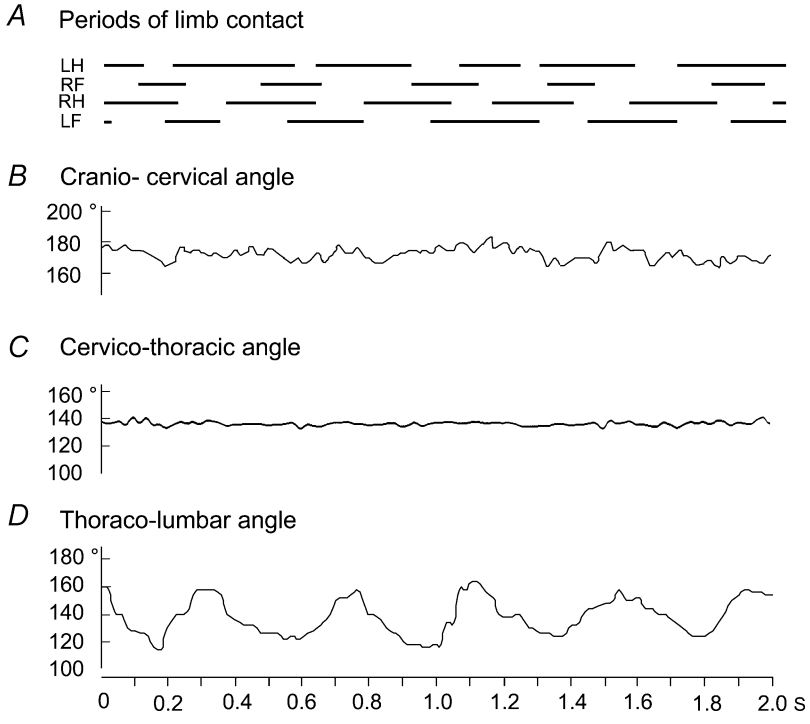

Figure 6. Skeletal movements of the circling IsK$^{-/-}$ mouse
The mouse was filmed from above while it made five counter-clockwise turns over 2 s (see Fig. 4*B*) Cineradiography film captured at 250 Hz and data sampling at 50 Hz. *A*, pattern of limb movement with same layout and abbreviations as Fig. 5*A*. RF, RH and LF exhibit a regular pattern in contrast to prolonged ground contact of the LH, which is used as a pivot. *B*, horizontal angle between the skull and the cervical column. *C*, horizontal angle between the cervical and thoracic columns. *D*, horizontal angle between the thoracic and lumbar columns. Note the stability of the front part of the body in contrast to the hind section.

bi-directional. Interestingly, with time we noticed that circling tended to become more unidirectional and this trend remains to be explained.

Why does the lack of functional horizontal canals provoke circling in IsK$^{-/-}$ mice? One possibility is that the resting discharge of the horizontal canal-related second-order vestibular neurones becomes inherently unstable following the disappearance of their afferent inputs. This is unlikely because at rest (i) the head of the IsK$^{-/-}$ mouse was stable in the horizontal plane, and (ii) their eyes did not display erratic or nystagmus-like movements in the dark. Alternatively, in quadrupeds, input from the horizontal semicircular canals could provide the feedback necessary to guide a planned trajectory. When this information is lacking, and IsK$^{-/-}$mice intend to change their heading direction, they continue to rotate for several turns. This proposal is consistent with the idea that perception of self-motion in humans incorporates vestibular information (Bloomberg *et al.* 1991; Israel *et al.* 1993). Finally, it is likely that other sources of sensory information (such as that sensed by the vibrissae) can substitute for the vestibular afferent inputs in more natural conditions, as IsK$^{-/-}$ mice are able to progress in plexiglass tubes (P.-P. Vidal, unpublished observations).

Vestibular information and motor development

Our results suggest that deprivation of vestibular information during development induces the behavioural syndromes of the IsK$^{-/-}$ mice. An important question is, at what developmental stage do vestibular deficits occurr? The IsK$^{-/-}$ mice could experience a congenital deprivation of vestibular information or, alternatively, their vestibular function could have been intact early on and then disappeared due to progressive labyrinth degeneration, inducing the circling behaviour around day 14 post gestation (P14). Histological evidence argues in favour of a congenital deficit. Collapse of the walls of the utriculus, sacculus and crista ampullaris, as well as the beginning of dark cell degeneration occurs as early as P3 (Vetter *et al.* 1996). The first signs of hair cell degeneration in the cristae are evident around P10. However, it could be argued that vestibular function was not totally impaired despite these histological signs. We think this is unlikely because as early as P7 the IsK$^{-/-}$ mice had unstable heads, they sometimes rolled spontaneously on their back, they had great difficulty recovering normal posture, and they could not swim. In addition, evidence that circling phenotype probably results from congenital rather than later vestibular deprivation comes from the finding that the continuous circling seen in the IsK$^{-/-}$ mice is not produced when both horizontal canals are plugged as early as P5 (Geisler & Gramsbergen, 1998). Consistent with this finding in mice is the fact that permanent circling has not been reported following bilateral vestibular lesions in any vertebrate species. Thus, taken together, these observations strongly suggest that vestibular function is severely impaired early in development in IsK$^{-/-}$ mice, and that this compromised postural and motor control before circling became an unequivocal indicator of the vestibular deficit.

Implications for motor control

A fundamental issue in the study of motor control is to understand how the CNS coordinates the large number of joints and muscles to achieve a common goal. There is kinematic redundancy in determining the position and orientation of the head relative to the trunk, as a great number of combinations of neck joint angles correspond to a given head position. At rest the skeletal system adopts a stereotyped S-shaped configuration in several mammalian

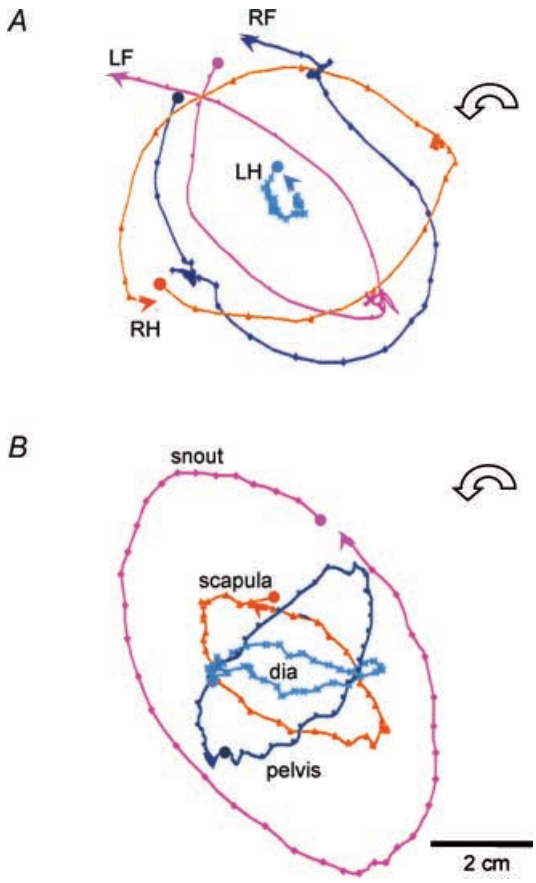

Figure 7. Trajectory of circling mouse
The IsK$^{-/-}$ mouse was filmed from above while it made five complete turns on wood surface (Fig. 4B). This figure illustrates the third turn. Cineradiography film captured at 250 Hz and data sampling at 50 Hz. *A*, trajectories in the horizontal plane of the extremities of the four limbs (abbreviations as in Fig. 5*A*). *B*, trajectories in the horizontal plane of the snout, the pelvis, the scapula and diaphragm (dia). The beginning and end of the trajectories are marked by circles and arrowheads, respectively.

species (Vidal *et al.* 1986, 1993; De Waele *et al.* 1989, 1990; Graf *et al.* 1992, 1995*a*,*b*; Selbie *et al.* 1993; Thomson *et al.* 1996; Keshner *et al.* 1997; Barberini & Macpherson, 1998; Macpherson & Ye, 1998; Statler & Keshner, 2003; Herbin *et al.* 2001). Here we show that mice are no exception in this regard. The S-shaped posture severely constrains motor control at rest: for instance, upward head movements cannot be implemented by a flexion at the cervico-thoracic junction as it is fully extended (∠ct, Fig. 3). Instead, such movements result from an extension of the atlanto-occipital joint (∠sc, Fig. 3), which is maximally flexed. The reverse is true for downward head movement. In addition, we observed a lack of lateral flexion between C2 and C6 (c, Fig. 3). Therefore, lateral flexion only takes place at the cervico-thoracic junction (∠ct, Fig. 3). It has been argued that an S-shaped posture is a favourable configuration to scan the horizon or to initiate an escape behaviour in any direction (Willock & Pearson, 1992). Thus, this S-shaped posture may have been selected by evolution because it is advantageous from a functional point of view while limiting the number of degrees of freedom that the CNS needs to control movement (Bernstein, 1947; Bizzi *et al.* 2000).

When skeletal geometry is modified from rest to trot, the degrees of freedom of the column are redistributed. At rest (Fig. 3), head and body horizontal rotations take place at the cervical and thoracic levels, respectively. These rotations cannot occur in the same way during trot due to the fully extended column (Fig. 4*A*). As the head maintains the same orientation at rest and during trot, a reconfiguration of the neuronal networks stabilizing these segments is required. This would mean that the same sensors, for example the horizontal semicircular canals, cannot control a given motoneurone pool in a similar way during these two motor behaviours.

Finally, our results reveal that an S-shaped skeletal geometry is not an exclusive attribute of the resting posture. Numerous studies in a variety of species of arthropods have shown that turning and curve walking are performed by changes in the timing and/or the structure of the stepping pattern of the legs (Franklin *et al.* 1981; Copp & Jamon, 2001). However, to our knowledge circling behaviour has not been the object of any study in vertebrates. As has been emphasized in several previous studies (Carrier *et al.* 2001; Higham *et al.* 2001; Lee *et al.* 2001; Walter & Carrier, 2002), the rotational inertia of the body is one of the main determinants of its turning performance. An S-shaped configuration during circling is beneficial in this regard, as it positions the head, neck and lumbar column close to the axis of rotation at the level of the centre of gravity. Accordingly, this strategy is likely to minimize the centrifugal forces on the animal during circling. This posture ensured that the heart was the most stable viscera during the rotation (please note the alignment of the heart of successive frames in Fig. 4*B*). Perhaps high and sustained centrifugal forces experienced by mice during sharp turns are detrimental to the cardiac system.

Conclusion

The fact that IsK$^{-/-}$ mice generate episodes of circling each time they try to change their heading direction suggests that vestibular inputs are required to signal the completion of their planned trajectory. We propose that, in particular, a lack of functional horizontal canals underlies this behaviour. Analogous situations in which subjects overshoot behavioural goals during self-motion have been described in previous reports. For example in cats, orientating head movements will significantly overshoot target location in the first few days that follow canal plugging (Fakhri *et al.* 1994). In addition, studies in humans and monkeys have reported marked head instability and hypermetric orientating movements immediately following vestibular loss (e.g. Dichgans *et al.* 1973; Maurer *et al.* 1998; Newlands *et al.* 1999). An important caveat regarding the circling phenotype in mice is that it is only stable if vestibular loss occurs very early in development as it does for IsK$^{-/-}$ mice. In humans, the congenital absence of labyrinthine function is initially associated with the delay of gross motor landmarks and balance functions. However, as children mature, the delay can be readily compensated for by the contribution of the proprioceptive, visual and motor systems. Nevertheless, some children remain significantly impaired and, for example, are unable to maintain static balance with eyes closed while swimming under water (Horak *et al.* 1988; Enbom *et al.* 1991; Admiraal & Huygen, 1997; Kaga, 1999). Thus, in contrast to mice, it seems likely that cognitive factors play a more significant role in determining how central pathways in humans integrate extra-vestibular information following vestibular loss in order to maintain posture and control movement.

References

Admiraal RJ & Huygen PL (1997). Vestibular areflexia as a cause of delayed motor skill development in children with the CHARGE association. *Int J Pediatr Otorhinolaryngol* **39**, 205–222.

Barberini CL & Macpherson JM (1998). Effect of head position on postural orientation and equilibrium. *Exp Brain Res* **122**, 175–184.

Bernstein NA (1947). *O Postroyeniis Dvizheniy* (On the construction of movements). Medgiz, Moscow. (English translation, *The Coordination and Regulation Of Movements*. Pergamon Press, Oxford, New York, 1967).

Bizzi E, Tresch MC, Saltiel P & d'Avella A (2000). New perspectives on spinal motor systems. *Nat Rev Neurosci* **1**, 101–108.

Bloomberg J, Melvill Jones G & Segal B (1991). Adaptive modification of vestibularly perceived rotation. *Exp Brain Res* **84**, 47–56.

Carrier DR, Walter RM & Lee DV (2001). Influence of rotational inertia on turning performance of theropod dinosaurs, clues from humans with increased rotational inertia. *J Exp Biol* **204**, 3917–3926.

Copp NH & Jamon M (2001). Kinematics of rotation in place during defense turning in the Crayfish procambarus clarkii. *J Exp Biol* **204**, 471–486.

Cullen KE & Roy JE (2004). Signal processing in the vestibular system during active versus passive head movements. *J Neurophysiol* **9**, 1919–1933.

Curthoys IS (2000). Vestibular compensation and substitution. *Curr Opin Neurol* **13**, 27–30.

Darlington CL, Dutia MB & Smith PF (2002). The contribution of the intrinsic excitability of vestibular nucleus neurons to recovery from vestibular damage. *Eur J Neurosci* **15**, 1719–1727.

De Waele C, Graf W, Josset P & Vidal P-P (1989). A radiological analysis of the postural syndromes following global and selective lesions in the guinea pig. *Exp Brain Res* **7**, 166–182.

de Waele C, Vibert N, Baudrimont M & Vidal P-P (1990). NMDA receptors contribute to the resting discharge of vestibular neurons in the normal and hemilabyrinthectomized guinea pig. *Exp Brain Res* **81**, 125–133.

Dichgans J, Bizzi E, Morasso P & Tagliasco V (1973). Mechanisms underlying recovery of eye-head coordination following bilateral labyrinthectomy in monkeys. *Exp Brain Res* **18**, 548–562.

Enbom H, Magnusson M & Pyykko I (1991). Postural compensation in children with congenital or early acquired bilateralvestibular loss. *Ann Otol Rhinol Laryngol* **100**, 472–478.

Fagerstedt P, Orlovsky GN, Deliagina TG, Grillner S & Ullen F (2001). Lateral turns in the Lamprey II activity of reticulospinal neurons during thegeneration of fictive turns. *J Neurophysiol* **86**, 2257–2265.

Fakhri S, Pelisson D & Guitton D (1994). Compensation for perturbations of gaze and role of vestibular signals in gaze control. In *Information Processing Underlying Gaze Control*, ed. Delgado-Garcia JM, Godaux E & Vidal PPL. Pergamon Press, New York/Oxford.

Franklin R, Bell WJ & Jander R (1981). Rotational locomotion by the cockroach Blatella germanica. *J Insect Physiol* **27**, 249–255.

Fung J & Macpherson JM (1999). Attributes of quiet stance in the chronic spinal cat. *J Neurophysiol* **82**, 3056–3065.

Geisler HC & Gramsbergen A (1998). Motor development after vestibular deprivation in rats. *Neurosci Biobehav Rev* **22**, 565–569.

Graf W, De Waele C & Vidal P-P (1992). Skeletal geometry in vertebrates and its relation to the vestibular endorgans. In *The Head-Neck Sensory–Motor System*, ed. Berthoz A, Graf W & Vidal P-P, pp. 129–134. Oxford University Press, New York, Oxford.

Graf W, De Waele C & Vidal P-P (1995*a*). Functional anatomy of the head-neck movement system of quadrupedal and bipedal mammals. *J Anat* **186**, 55–74.

Graf W, De Waele C, Vidal P-P, Wang D-H & Evinger C (1995*b*). The orientation of the cervical vertebral column in unrestrained awake animals II movement strategies. *Brain Behav Evol* **45**, 209231.

Gray LE, Rogers JM, Ostby JS, Kavlock RJ & Ferrell JM (1988). Prenatal dinocarp exposures alters swimming behavior in mice due to complete otolith agenesis in the inner ear. *Toxicol Appl Pharmacol* **92**, 266–273.

Hayes AV, Richmond BJ & Optican LM (1982). A UNIX-based multiple process system for real-time data acquisition and control. *WESCON Conf Pro* **2**, 1–10.

Herbin M, Jeanne V, Gasc JP & Vidal P-P (2001). Skeletal configurations of cervical column during rest to motion transition, generalization that underlies the motor repertoire in rodents. *C R Acad Sci III* **324**, 45–50.

Higham TE, Davenport MS & Jayne BC (2001). Maneuvering in an arboreal habitat, the effects of turning angle on the locomotion of three sympatric ecomorphs of Anolis lizards. *J Exp Biol* **204**, 4141–4155.

Horak FB, Shumway-Cook A, Crowe TK & Black FO (1988). Vestibular function and motor proficiency of children with impaired hearing, or with learning disability and motor impairments. *Dev Med Child Neurol* **30**, 64–79.

Hunt MA, Miller SW, Nielson HC & Horn KM (1987). Intratympanic injection of sodium arsanilate (atoxyl) solution results in postural changes consistent with changes described for labyrinthectomized rats. *Behav Neurosci* **101**, 427–428.

Israel I, Fetter M & Koenig E (1993). Vestibular perception of passive whole-body rotation about horizontal and vertical axes in humans, goal-directed vestibulo-ocular reflex and vestibular memory-contingent saccades. *Exp Brain Res* **96**, 335–346.

Iwashita M, Kanai R, Funabiki K, Matsuda K & Hirano T (2001). Dynamic properties, interactions and adaptive modifications of vestibulo-ocular reflex and optokinetic response in mice. *Neurosci Res* **39**, 299–311.

Kaga K (1999). Vestibular compensation in infants and children with congenital and acquired vestibular loss in both ears. *Int J Pediatr Otorhinolaryngol* **49**, 215–224.

Kaiser A, Fedrowitz M, Ebert U, Zimmermann E, Hedrich HJ, Wedekind D & Loscher W (2001). Auditory and vestibular defects in the circling (ci2) rat mutant. *Eur J Neurosci* **14**, 1129–1142.

Keshner EA, Statler KD & Delp SL (1997). Kinematics of the freely moving head and neck in the alert cat. *Exp Brain Res* **115**, 257–266.

Lee DV, Walter RM, Deban SM & Carrier DR (2001). Influence of increased rotational inertia on the turning performance of humans. *J Exp Biol* **204**, 3927–3934.

Letts VA, Valenzuela A, Dunbar C, Zheng QY, Johnson KR & Frankel WN (2000). A new spontaneous mouse mutation in the *Kcne1* gene. *Mamm Genome* **11**, 831–835.

Macpherson JM & YeY (1998). The cat vertebral column, stance configuration and range of motion. *Exp Brain Res* **119**, 324–332.

Maurer C, Mergner T, Becker W & Jurgens R (1998). Eye-head coordination in labyrinthine-defective humans. *Exp Brain Res* **122**, 260–274.

Newlands SD, Ling L, Phillips JO, Siebold C, Duckert L & Fuchs AF (1999). Short- and long-term consequences of canal plugging on gaze shifts in the rhesus monkey. I. Effects on gaze stabilization. *J Neurophysiol* **81**, 2119–2130.

Nicolas M, Dememes D, Martin A, Kupershmidt S & Barhanin J (2001). KCNQ1/KCNE1 potassium channels in mammalian vestibular dark cells. *Hearing Res* **153**, 132–145.

Ossenkopp KP, Prkacin A & Hargreaves EL (1990). Sodium arsenilate-induced vestibular dysfunction in rats, effects on openfield behavior and spontaneous activity in the automated digiscan monitoring system. *Parmacol Biochem Behav* **36**, 875–881.

Rabbath G, Necchi D, de Waele C, Gasc JP, Josset P & Vidal P-P (2001). Abnormal vestibular control of gaze and posture in a strain of a waltzing rat. *Exp Brain Res* **136**, 211–223.

Renous S (1994). *Locomotion Edition.* Dunod, Paris.

Selbie WS, Thomson DB & Richmond FJ (1993). Sagittal-plane mobility of the cat cervical spine. *J Biomech* **26**, 917–927.

Shoham S, Chen Y-C, Devietti TL & Teitelbaum P (1989). Deafferentation of the vestibular organ, effects on atropine-resistant EEG in rats. *Psychobiol* **17**, 307–314.

Stahl JS (2002). Calcium channelopathy mutants and their role in ocular motor research. *Ann N Y Acad Sci* **956**, 64–74.

Stahl JS, Van Alphen AM & de Zeeuw CL (2000). A comparison of video and magnetic search coil recordings of mouse eye movements. *J Neurosci Methods* **99**, 101–110.

Statler KD & Keshner EA (2003). Effects of inertial load and cervical-spine orientation on a head-tracking task in the alert cat. *Exp Brain Res* **148**, 202–210.

Takumi T, Ohkubo H & Nakanishi S (1988). Cloning of a membrane protein that induces a slow voltage-gated potassium current. *Science* **242**, 1042–1045.

Thomson DB, Loeb GE & Richmond FJ (1996). Effect of neck posture on patterns of activation of feline neck muscles during horizontal rotation. *Exp Brain Res* **110**, 392–400.

Vetter DE, Mann J-R, Wangemann P, Liu J, McLaughlin K-J, Lesage F, Marcus D-C, Lazdunsk M, Heinemann S-F & Barhanin J (1996). Inner ear defects induced by null mutation of the IsK gene. *Neuron* **17**, 1251–1264.

Vidal P-P, de Waele C, Vibert N & Muhlethaler M (1998). Vestibular compensation revisited. *Otolaryngol Head Neck Surg* **119**, 34–42.

Vidal P-P, Graf W & Berthoz A (1986). The orientation of the cervical vertebral column in unrestrained awake animals. I. Resting position. *Exp Brain Res* **61**, 549–559.

Vidal P-P, Wang D-H, Graf W & de Waele C (1993). Vestibular control of skeletal geometry in the guinea pig, a problem of good trim? *Prog Brain Res* **97**, 229–243.

Walter RM & Carrier DR (2002). Scaling of rotational inertia in murine rodents and two species of lizard. *J Exp Biol* **205**, 2135–2341.

Warth R & Barhanin J (2002). The multifaceted phenotype of the knockout mouse for the KCNE1 potassium channel gene. *Am J Physiol Regul Integr Comp Physiol* **282**, R639–R648.

Wersäll J & Hawkins EJ (1962). The vestibular sensory epithelia in the cat labyrinth and their reactions in chronic streptomycin intoxication. *Acta Otolaryngol (Stockholm)* **54**, 1–23.

Willock C & Pearson J (1992). *Predators of the Wild*, vol. 6. Warner House Video, Burbank, CA, USA.

Acknowledgements

We thank J. Roubertoux and J. Barhanin who provided us with the mutant mice. We thank also C. de Waele and I. Vassias for performing the unilateral labyrinthectomy in the mice and C. Magnani for excellent technical assistance. We thank L. Moore and the reviewing editor for their help in greatly improving the manuscript. This research was supported by grants from the CNRS, Paris 5, the Museum National d'Histoire Naturelle, the Centre National d'Etudes Spatiales and the McGill Dawson Chair Program.